Late Stage Diversification of an Unsymmetrical Ligand Scaffold for Multi-functional *cis*-Pd_2L_4 Nanocage Libraries

James E. M. Lewis*

Dr. J. E. M. Lewis
Department of Chemistry
Imperial College London
Molecular Sciences Research Hub, 82 Wood Lane, London W12 0BZ
*E-mail: james.lewis@imperial.ac.uk

Abstract

Although many impressive metallo-supramolecular architectures have been reported, they tend towards high symmetry structures and avoid extraneous functionality to ensure high-fidelity in the self-assembly process. This minimalist approach, however, limits the range of accessible structures and thus their potential applications. Herein is described a late stage diversification strategy towards ligand scaffolds that are both low symmetry and incorporate exohedral functional moieties. Key to this design is the use of CuAAC chemistry, as the triazole is capable of acting as both a coordinating heterocycle and a tether between the ligand framework and functional unit simultaneously. In this manner a common precursor was used to generate ligands with various functionalities, allowing control of electronic properties, whilst maintaining the core structure of the resultant *cis*-Pd_2L_4 nanocage assemblies. The isostructural nature of the scaffold frameworks enabled formation of combinatorial libraries from the self-assembly of ligand mixtures, generating multi-functional, low-symmetry architectures.

Introduction

The self-assembly of metal-organic polyhedra (MOPs)[1] remains a popular tool for supramolecular chemists to generate intricate architectures, from minimalist building blocks, that have demonstrated myriad functionality.[2] Simplicity of components is advantageous: symmetrical structures mitigate the competing processes of *narcissistic* (self-recognition) and *integrative* self-sorting (heteromeric-assembly),[3] whilst minimalist ligands inhibit potentially disruptive effects from functional units. Trading fidelity of assembly for high-symmetry and spartan scaffolds, however, limits the scope for developing more sophisticated systems.

Pd_2L_4 molecular cages[4] have become a common class of MOP and, despite the potential impediments, strategies for accessing lower symmetry variants have been reported. Use of steric[5] and geometric[6] parameters has enabled the self-assembly of heteroleptic[7] dipalladium nanocages. Exploiting coordination preferences to generate stable metallo-ligands[8] has allowed mixed-metal architectures[9] to be realised. Work in this group,[10] and by others,[11] has focused on an alternative, underexplored option: the use of low-symmetry ligands.[12] Designed such that steric or geometric parameters, or a combination of the two, direct the self-assembly process, exclusive formation of specific cage isomers from a potential mixture can be ensured. Although these concepts have been successfully employed in the formation of reduced symmetry MOPs, they remain devoid of functionality. Indeed, research into exohedral[13] and endohedral[14] functionalisation of ligand scaffolds for MOPs altogether remains relatively scarce.

The 1,2,3-triazole, most commonly synthesised using the Cu(I)-catalysed azide-alkyne cycloaddition (CuAAC) reaction,[15] has become a ubiquitous unit in supramolecular chemistry.[16] In addition to being the coordinating unit in readily accessible ligands for MOPs,[17] the specificity of the CuAAC reaction makes the triazole ideal as a benign linker between coordinating and functional moieties.[18] Routinely utilised in either of these roles, the function of the triazole is usually determined at an early stage in the design process. Furthermore, the ability of the triazole to fulfil both of these mandates simultaneously is rarely exploited.

Late stage functionalisation is a strategy commonly employed in medicinal chemistry to diversify a lead structure and generate an array of analogues.[19] It was considered that this philosophy could be applied to a proto-ligand scaffold for MOPs, allowing a family of ligands to be generated from a common precursor. This report details the use of unsymmetrical, mixed-heterocycle ditopic ligands, with isoquinoline and 1,2,3-triazole coordinating units, for the formation of functionalised *cis*-Pd_2L_4 architectures. Introduction of the triazole unit as the final step in the ligand synthesis enables late stage diversification of a common precursor, allowing tuning of ligand properties, whilst maintaining the structure of the framework core. This structural consistency was able to be exploited in the assembly of mixed-ligand combinatorial cage libraries.

Results and Discussion

Based on principles delineated from earlier work,[10] ligand $\mathbf{L^R}$ (Scheme 1a), envisaged to be derived from an azide precursor, was designed incorporating both isoquinoline and triazole coordinating units. Optimised models from semi-empirical calculations (PM6) of the four potential $[Pd_2\mathbf{L}_4]^{4+}$ cage isomers assembled from the hypothetical $\mathbf{L^{Me}}$ (where R = CH_3) indicated that the *cis*-Pd_2L_4 isomer would be lowest in energy (Scheme 1b), consistent with previous computational and experimental work.[11] Furthermore, the optimised structure of the *cis* isomer displayed no disquieting distortions of common structural parameters such as N-Pd-N (~176°) or alkyne (~179°) angles to suggest its formation would be unfavourable.

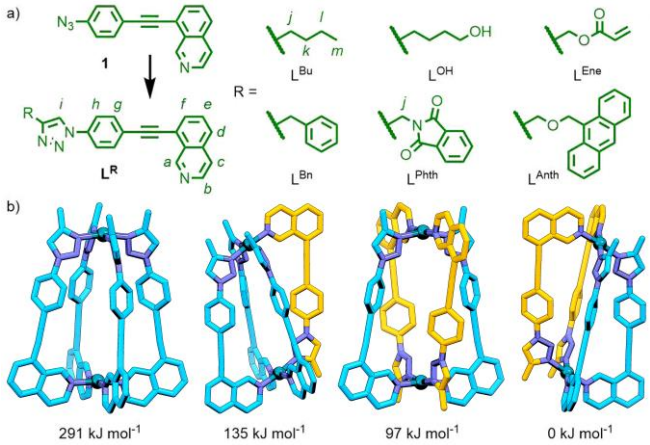

Scheme 1. a) Synthesis of ligands, $\mathbf{L^R}$, from azide precursor **1**. b) Geometry optimised structures (PM6) of the four potential $[Pd_2(\mathbf{L^{Me}})_4]^{4+}$ isomers and their relative energies (from left to right: "all-up", "three-up-one-down", *trans* and *cis*). Orange and blue colouring denotes relative ligand orientation.

Buoyed by these rudimentary computational results, the ligand precursor, **1**, was prepared in 86% overall yield from commercially available reagents (see Supporting Information for details). Submission of **1** to standard CuAAC reaction conditions ($CuSO_4{\cdot}5H_2O$, sodium ascorbate, DMF, rt) with 1-hexyne gave $\mathbf{L^{Bu}}$ in 89% yield.

Pleasingly, a 2:1 combination of $\mathbf{L^{Bu}}$ with $[Pd(CH_3CN)_4](BF_4)_2$ in d_6-DMSO resulted in a sharp ^{1}H NMR spectrum composed of a single set of signals (Fig. 1a). The combination of downfield shifts of isoquinoline (H_a and H_b; $\Delta\delta$ = 0.50 and 1.25 ppm, respectively) and triazole (H_i; $\Delta\delta$ = 0.37 ppm) signals in the ^{1}H NMR spectrum (Fig. S42), calculated solvodyanamic radius (R_S; 9.7 Å) from diffusion-ordered NMR spectroscopy (DOSY; $D = 1.03 \times 10^{-10}$ m^{2}s^{-1}), and signals observed by mass spectrometry (MS; Fig. 1b) all indicated formation of a species with formula $[Pd_2(\mathbf{L^{Bu}})_4]^{4+}$. The symmetry of the ^{1}H NMR spectrum and cross-peaks observed by NOESY ($H_b{\cdots}H_j$; Fig 1c) determined that either the *cis* or *trans* isomer had been obtained. Diastereotopic splitting of methylene units of the butyl chain (H_j and H_k) suggested that the *cis* isomer was most likely to have formed. Ultimately, unambiguous confirmation of the *cis*-$[Pd_2(\mathbf{L^{Bu}})_4]^{4+}$ structure came from solid state single-crystal X-ray diffraction (SCXRD) data (Fig. 1d and e).

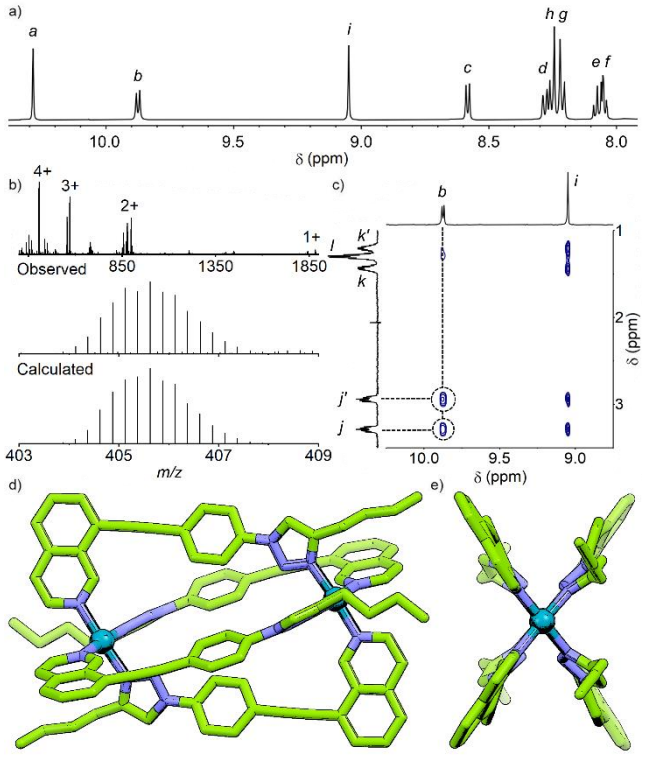

Figure 1. a) Partial ^{1}H NMR spectrum (500 MHz, d_6-DMSO, 298 K) of $[Pd_2(\mathbf{L^{Bu}})_4](BF_4)_4$; b) MS with observed and calculated peak for $[Pd_2(\mathbf{L^{Bu}})_4]^{4+}$; c) partial NOESY spectrum showing through-space interactions between isoquinoline H_b and butyl chain H_j signals (for signal labelling see Scheme 1); SCXRD structure of $[Pd_2(\mathbf{L^{Bu}})_4](BF_4)_4$ shown d) from the side, and e) down the Pd-Pd axis. N-Pd bond lengths 2.022-2.032 Å; N-Pd-N angles 176.2-176.3°; Pd···Pd distance 11.1 Å. Counterions, solvent molecules and hydrogen atoms omitted for clarity.

Having shown that the ligand framework was indeed suitable for the specific formation of *cis*-Pd_2L_4 structures, a number of ligands derived from the common precursor **1** were prepared (Scheme 1a). In addition to alkyl substituents, self-assembly of the ligand framework with Pd(II) was found to be compatible with aryl ($\mathbf{L}^{\mathbf{Bn}}$) and bulkier aromatic ($\mathbf{L}^{\mathbf{Anth}}$) and heterocyclic ($\mathbf{L}^{\mathbf{Phth}}$) moieties, as well as substituents containing heteroatoms ($\mathbf{L}^{\mathbf{OH}}$) and unsaturated units ($\mathbf{L}^{\mathbf{Ene}}$). Similar MS and NMR spectroscopic details (see Supporting Information) for each of these assemblies indicated no alteration in the preference for formation of *cis*-Pd_2L_4 cage isomers. With the core *cis*-Pd_2L_4 framework remaining isostructural amongst the ligands examined (Figure 2), the ability to use the triazole substituents to modify the properties of the assemblies was investigated.

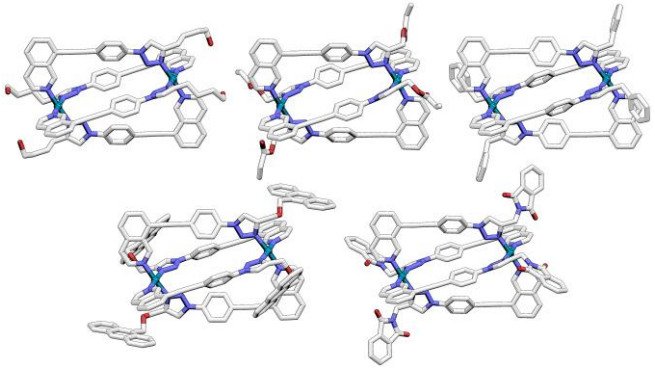

Figure 2. Optimised structures (PM6) of *cis*-$[Pd_2(\mathbf{L}^{\mathbf{R}})_4]^{4+}$ cages assembled from (clockwise from top left) $\mathbf{L}^{\mathbf{OH}}$, $\mathbf{L}^{\mathbf{Ene}}$, $\mathbf{L}^{\mathbf{Bn}}$, $\mathbf{L}^{\mathbf{Phth}}$ and $\mathbf{L}^{\mathbf{Anth}}$. Hydrogen atoms omitted for clarity.

Although generally considered to be weaker ligands than pyridines, the electronic properties of 1,2,3-triazoles can be tuned with precision through varying the C- and N-substituents.[20] The potential for fine tuning the ligand strength of triazoles in metallo-supramolecular systems, however, is largely overlooked.[21] Within the current system, modulation of donor strength was demonstrated through a comparison of the self-assembly profiles of ligands $\mathbf{L}^{\mathbf{Bu}}$ and $\mathbf{L}^{\mathbf{Phth}}$ incorporating electron-donating and -withdrawing groups, respectively.

Titration of Pd(II) into a d_6-DMSO solution of $\mathbf{L}^{\mathbf{Phth}}$ (Fig. 3a) resulted in formation of the expected $[Pd_2(\mathbf{L}^{\mathbf{Phth}})_4]^{4+}$ cage when a 1:2 metal/ligand ratio was reached (Fig. 3c). At a 1:4 ratio, however, a single species was observed (Fig. 3b) that was spectroscopically distinct from both the free ligand and Pd_2L_4 cage, although DOSY suggested that it was of a similar size to the latter ($R_S \approx 11$ Å, compared to 11.3 Å for the cage). The NOESY spectrum (Fig. S109) revealed cross-peaks between H_a and H_b of the isoquinoline, which would only be expected were at least two of these heterocycles to be brought into close proximity through coordination in an anti-parallel fashion (Fig. 3g); in contrast to the cage, *cis*-$[Pd_2(\mathbf{L}^{\mathbf{Phth}})_4]^{4+}$, no interactions between H_b of the isoquinoline and H_j of the triazole substituent were observed (Fig. 3h). These data are consistent with the formation of a mononuclear complex, $[Pd(\mathbf{L}^{\mathbf{Phth}})_4]^{2+}$, with coordination to the Pd(II) ions occurring through the isoquinoline units (Fig. 3i).

Additional support for the identity of the mononuclear species came from a model compound, namely the complex formed from the self-assembly of monodentate ligand precursor **1**. A 4:1 mixture of **1** with Pd(II) yielded a sharp set of signals (Fig. S113) wherein characteristic peaks - H_a, H_b and H_g - resonated at similar chemical shifts to those observed for the purported $[Pd(\mathbf{L}^{\mathbf{Phth}})_4]^{2+}$ complex. Unfortunately, no signals for this latter species were observed by MS (although an isotopic pattern consistent with the formula $\{[Pd(\mathbf{L}^{\mathbf{Phth}})_3](X^-)\}^+$ (Fig. S111) could be seen), presumably due to the instability of the mononuclear complex under the ESI-MS conditions.

The situation with $\mathbf{L}^{\mathbf{Bu}}$ was slightly more complex. The ^{1}H NMR spectrum obtained from a 1:4 mixture of Pd(II) and $\mathbf{L}^{\mathbf{Bu}}$ (Fig. 3f) at first glance appeared to indicate a stoichiometric mixture of $[Pd_2(\mathbf{L}^{\mathbf{Bu}})_4]^{4+}$ (Fig. 3d) and free $\mathbf{L}^{\mathbf{Bu}}$ (Fig. 3e). Closer inspection revealed additional peaks, belonging to neither of these species, that resembled the mononuclear complex seen with $\mathbf{L}^{\mathbf{Phth}}$. This suggested that these three species ($\mathbf{L}^{\mathbf{Bu}}$, $[Pd(\mathbf{L}^{\mathbf{Bu}})_4]^{2+}$ and $[Pd_2(\mathbf{L}^{\mathbf{Bu}})_4]^{4+}$) might all be present in solution.

2D NMR – in particular NOESY and DOSY – was used to assign non-overlapping signals to individual components of this mixture. In the NOESY spectrum cross-peaks indicative of $H_b \cdots H_j$ interactions between the isoquinoline and butyl chain (Fig. 3h) could be seen for the cage assembly but were absent for those signals assigned to the mononuclear complex; additionally $H_a \cdots H_b$ interactions could be seen for the latter (Fig. 3g). DOSY showed peaks assigned to the cage and mononuclear complexes to be diffusing at similar rates (D = 10.0 and 9.8 × 10^{-11} m^2s^{-1}, respectively) whilst those assumed to be from the free ligand diffused much quicker (D = 4.4 × 10^{-11} m^2s^{-1}), indicative of two similarly sized species and one much smaller (R_S = 10.3, 9.7 and 4.4 Å, respectively) being present in solution.

Thus, based on the spectral data, it was concluded that a 1:4 mixture of Pd(II) and $\mathbf{L}^{\mathbf{Bu}}$ generated a combination of the dinuclear cage, mononuclear complex (with coordination again presumed to be through the isoquinoline units) and free ligand. It is noted that for free $\mathbf{L}^{\mathbf{Bu}}$, downfield signals associated with protons H_a and H_b adjacent to the nitrogen atom of the isoquinoline could not be identified. It is assumed that these peaks had broadened significantly, possibly due to transient non-covalent interactions with the $[Pd_2(\mathbf{L}^{\mathbf{Bu}})_4]^{4+}$ and/or $[Pd(\mathbf{L}^{\mathbf{Bu}})_4]^{2+}$ complexes.

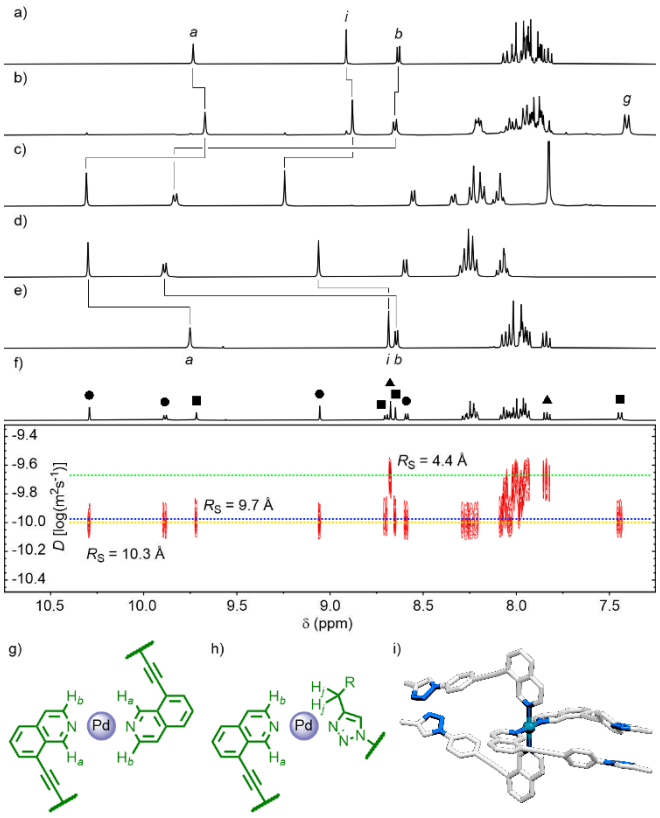

Figure 3. Controlling the self-assembly profile of $\mathbf{L^R}$ through tuning the electronic properties of the triazole. Partial ^{1}H NMR spectra (400 MHz, d_6-DMSO, 298 K) of a) $\mathbf{L^{Phth}}$, b) $\mathbf{L^{Phth}}$ + 0.25 eq. Pd(II), c) $\mathbf{L^{Phth}}$ + 0.50 eq. Pd(II), d) $\mathbf{L^{Bu}}$ + 0.50 eq. Pd(II), and e) $\mathbf{L^{Phth}}$. For signal labelling see Scheme 1. f) Partial DOSY spectrum (500 MHz, d_6-DMSO, 298 K) of $\mathbf{L^{Phth}}$ + 0.25 eq. Pd(II). Non-overlapping peaks have been assigned where possible as $[Pd_2(\mathbf{L^{Bu}})_4]^{4+}$ (●), $[Pd(\mathbf{L^{Bu}})_4]^{2+}$ (■), and $\mathbf{L^{Bu}}$ (▲). Chemical structures showing indicative through-space interactions between protons for g) mononuclear $[Pd(\mathbf{L^R})_4]^{2+}$ species, and h) $[Pd_2(\mathbf{L^R})_4]^{4+}$ cage assemblies. i) Molecular model of one possible conformation of a mononuclear $[Pd(\mathbf{L^{Me}})_4]^{2+}$ structure with coordination exclusively through the isoquinoline units.

The proton affinity (PA) of N3 of the triazole, as determined by DFT calculations (B3LYP-6-31G(d)), was increased by 16 kJ mol^{-1} going from the electron-withdrawing N-methylenephthalimide substituent in $\mathbf{L^{Phth}}$ to the electron-donating butyl group of $\mathbf{L^{Bu}}$ (see Supporting Information for details). Using PA as a proxy for ligand strength, these results support the rationalisation of the observed differences in self-assembly as arising from differences in the σ-donor ability of the triazoles between the two ligands. The combined experimental and computational results demonstrate effective control of the ligand framework's electronic properties, through tailoring of the triazole substituent, without ultimately affecting the core structure of the *cis*-Pd_2L_4 assembly.

Since the core framework remained constant between the different functionalised ligands, it seemed that it would be possible to generate a statistical combinatorial library of homoleptic and mixed-ligand cages through self-assembly of a mixture of more than one ligand.[22] To examine this, Pd(II) and a binary mixture of $\mathbf{L^{Bu}}$ and either $\mathbf{L^{Bn}}$ or $\mathbf{L^{Phth}}$ were combined in a 1:1:1 ratio in d_6-DMSO. The resultant self-assembled libraries gave well-defined ^{1}H NMR spectra (Fig. 4b and S115) that appeared to contain multiple overlapping signals from species of a similar size to the homoleptic assemblies ($R_S \approx$ 10-11 Å). These mixtures were found to be composed of the five possible homoleptic and heteroleptic constitutional assemblies with the formula $[Pd_2(\mathbf{L^{Bu}})_x(\mathbf{L^{Bn}}/\mathbf{L^{Phth}})_{(4-x)}]^{4+}$ (Fig. 4d) by MS (Fig. 4e).

It is noted that whilst the homoleptic and *cis*-$Pd_2\mathbf{L^1}_3\mathbf{L^2}$-type architectures should be present as single diastereomers, *cis*-$Pd_2\mathbf{L^1}_2\mathbf{L^2}_2$ assemblies with unsymmetrical ligands have the potential to exist as three different diastereomeric forms depending on the relative arrangements and orientations of the ligands (Fig. 4d), although these isomers cannot be distinguished by MS. Additionally the two $Pd_2\mathbf{L^1}_3\mathbf{L^2}$ and one of the $Pd_2\mathbf{L^1}_2\mathbf{L^2}_2$ cages are chiral, resulting in a library of ten cages in total. Herein the three $Pd_2\mathbf{L^1}_2\mathbf{L^2}_2$ cage isomers have been termed syn, *cis*-anti and *trans*-anti, where for pairs of the same ligand (in this instance e.g. the pair of $\mathbf{L^{Bu}}$ ligands) syn/anti denotes parallel/antiparallel relative orientations, and *cis*/*trans* indicates their relative positions within the *cis*-Pd_2L_4 structure (i.e. adjacent or opposite from each other, respectively).

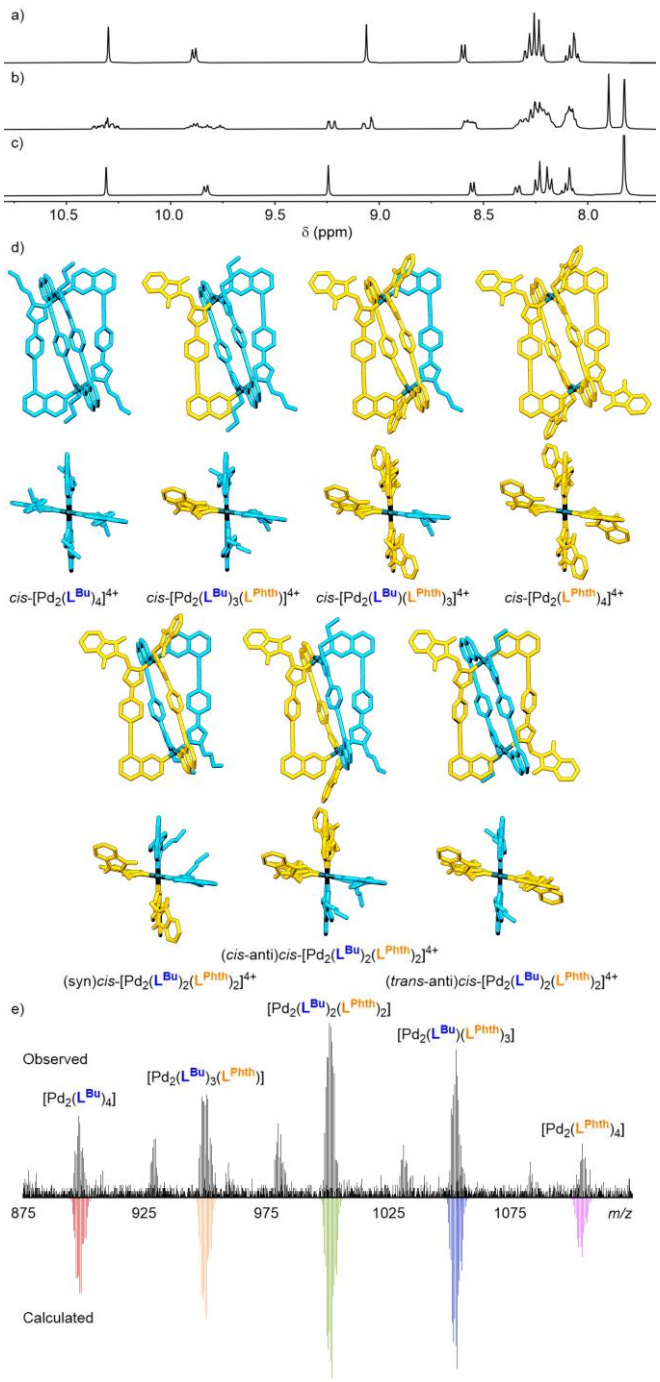

Figure 4. Partial ^{1}H NMR spectra (400 MHz, d_6-DMSO, 298 K) of a) $[Pd_2(\mathbf{L^{Bu}})_4](BF_4)_4$, b) combinatorial library $[Pd_2(\mathbf{L^{Bu}})_x(\mathbf{L^{Phth}})_{(4-x)}](BF_4)_4$, and c) $[Pd_2(\mathbf{L^{Phth}})_4](BF_4)_4$. d) Optimised structures (PM6) of the members of the combinatorial library $[Pd_2(\mathbf{L^{Bu}})_x(\mathbf{L^{Phth}})_{(4-x)}]^{4+}$ including the three isomeric forms of $[Pd_2(\mathbf{L^{Bu}})_2(\mathbf{L^{Phth}})_2]^{4+}$. $\mathbf{L^{Bu}}$ and $\mathbf{L^{Phth}}$ ligands have been coloured blue and orange, respectively. e) Observed MS and calculated signals for $\{[Pd_2(\mathbf{L^{Bu}})_x(\mathbf{L^{Phth}})_{(4-x)}](BF_4)_2\}^{2+}$ ions (x = 0-4).

Having successfully demonstrated statistical mixing of a binary combination of ligands, a ternary system was subsequently examined. $\mathbf{L^{OH}}$, $\mathbf{L^{Phth}}$ and $\mathbf{L^{Anth}}$ were combined with Pd(II) in a 2:2:2:3 ratio in d_6-DMSO. Unsurprisingly the resultant ^{1}H NMR spectrum was somewhat complex (Fig. S123). The DOSY data, however, was consistent with the formation of appropriately sized assemblies (R_S = 11.0 Å) and MS confirmed the presence of the three possible tris-heteroleptic assemblies (i.e. those incorporating at least one of each ligand) (Fig. 5a-c). Signals consistent with most of the 15 expected constitutional assemblies of the library could also be seen (Fig. 5d). As several of the bis-heteroleptic and all of the tris-heteroleptic assemblies are expected to exist as a mixture of diastereomers, and a number of these are chiral, the combinatorial library is considered to consist of a total of 47 *cis*-Pd_2L_4 cages (Fig. S128).

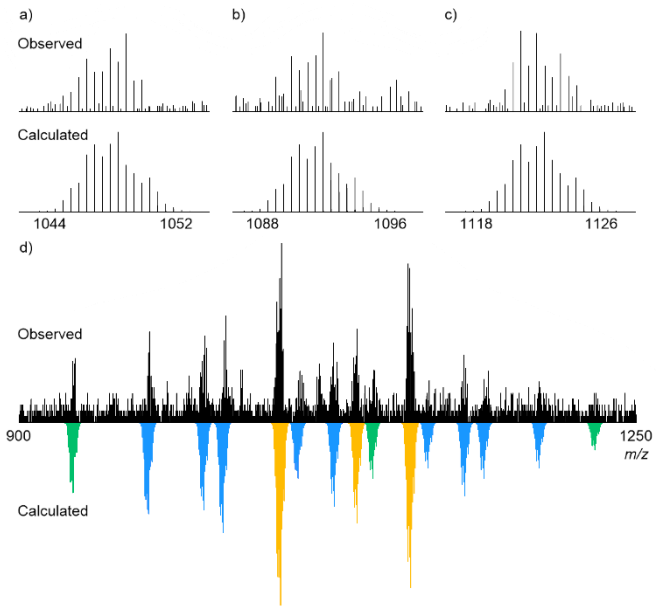

Figure 5. Observed and calculated MS patterns for a) $\{[Pd_2(\mathbf{L}^{\mathbf{OH}})_2(\mathbf{L}^{\mathbf{Phth}})(\mathbf{L}^{\mathbf{Anth}})](BF_4)_2\}^{2+}$, b) $\{[Pd_2(\mathbf{L}^{\mathbf{OH}})(\mathbf{L}^{\mathbf{Phth}})_2(\mathbf{L}^{\mathbf{Anth}})](BF_4)_2\}^{2+}$, and c) $\{[Pd_2(\mathbf{L}^{\mathbf{OH}})(\mathbf{L}^{\mathbf{Phth}})(\mathbf{L}^{\mathbf{Anth}})_2](BF_4)_2\}^{2+}$. d) Partial MS of the ternary combinatorial library with calculated signals for $\{[Pd_2L_4](BF_4)_2\}^{2+}$ ions with one (green), two (blue), and three (orange) different ligands.

Conclusions

In conclusion, a late stage diversification strategy has been used to generate unsymmetrical, ditopic ligands that self-assemble into exohedrally-functionalised, low-symmetry *cis*-Pd_2L_4 architectures. CuAAC chemistry was employed to yield mixed-heterocycle ligands in which a 1,2,3-triazole unit served as both a coordinating unit and linker to append functional groups to the assembly scaffold. A variety of functional groups were shown to be tolerated without impacting the core structure of the cage. Furthermore, facile tuning of electronic properties was demonstrated, allowing modification of the ligand self-assembly profile. Due to the isostructural nature of the core framework of the ligands, and their resultant Pd_2L_4 assemblies, it was shown possible to generate combinatorial libraries that included mixed-ligand architectures with multiple functional moieties. With the need to move towards more complex MOPs in order to advance their utility in various applications, this study has demonstrated an underexplored approach to readily access functional, low-symmetry metal-organic assemblies.

Acknowledgements

This work was supported by an Imperial College Research Fellowship. Thanks to Peter Haycock and Corey Fulop for assistance with the collection of NMR data, Dr Lisa Haigh for MS data, Dr Andrew White for collection of SCXRD data, Dr Dan Preston for useful discussions, and Prof. Matthew Fuchter for useful discussions and access to equipment and resources.

References & Notes

For calculated structures in xyz format see DOI:10.14469/hpc/7559.

[1] a) M. Fujita, *Chem. Soc. Rev.* **1998**, *27*, 417–425; b) S. Leininger, B. Olenyuk, P. J. Stang, *Chem. Rev.* **2000**, *100*, 853–908; c) B. J. Holliday, C. A. Mirkin, *Angew. Chem. Int. Ed.* **2001**, *40*, 2022–2043; d) M. D. Ward, *Chem. Commun.* **2009**, 4487–4499; e) R. Chakrabarty, P. S. Mukherjee, P. J. Stang, *Chem. Rev.* **2011**, *111*, 6810–6918; f) M. M. J. Smulders, I. A. Riddell, C. Browne, J. R. Nitschke, *Chem. Soc. Rev.* **2013**, *42*, 1728–1754; g) T. K. Ronson, S. Zarra, S. P. Black, J. R. Nitschke, *Chem. Commun.* **2013**, *49*, 2476–2490; h) T. R. Cook, P. J. Stang, *Chem. Rev.* **2015**, *115*, 7001–7045; i) N. B. Debata, D. Tripathy, H. S. Sahoo, *Coord. Chem. Rev.* **2019**, *387*, 273–298.

[2] a) M. Yoshizawa, J. K. Klosterman, M. Fujita, *Angew. Chem. Int. Ed.* **2009**, *48*, 3418–3438; b) T. R. Cook, V. Vajpayee, M. H. Lee, P. J. Stang, K. W. Chi, *Acc. Chem. Res.* **2013**, *46*, 2464–2474; c) B. Therrien, *Chem. - Eur. J.* **2013**, *19*, 8378–8386; d) C. J. Brown, F. D. Toste, R. G. Bergman, K. N. Raymond, *Chem. Rev.* **2015**, *115*, 3012–3035; e) A. Casini, B. Woods, M. Wenzel, *Inorg. Chem.* **2017**, *56*, 14715–14729; f) T. Y. Kim, R. A. S. Vasdev, D. Preston, J. D. Crowley, *Chem. - Eur. J.* **2018**, *24*, 14878–14890; g) I. Sinha, P. S. Mukherjee, *Inorg. Chem.* **2018**, *57*, 4205–4221; h) Y. Fang, J. A. Powell, E. Li, Q. Wang, Z. Perry, A. Kirchon, X. Yang, Z. Xiao, C. Zhu, L. Zhang, et al., *Chem. Soc. Rev.* **2019**, *48*, 4707–4730; i) H. Sepehrpour, W. Fu, Y. Sun, P. J. Stang, *J. Am. Chem. Soc.* **2019**, *141*, 14005–14020; j) F. J. Rizzuto, L. K. S. von Krbek, J. R. Nitschke, *Nat. Rev. Chem.* **2019**, *3*, 204–222; k) E. J. Gosselin, C. A. Rowland, E. D. Bloch, *Chem. Rev.* **2020**, *120*, 8987–9014; l) Y. Xue, X. Hang, J. Ding, B. Li, R. Zhu, H. Pang, Q. Xu, *Coord. Chem. Rev.* **2020**, DOI 10.1016/j.ccr.2020.213656.

[3] a) Z. He, W. Jiang, C. A. Schalley, *Chem. Soc. Rev.* **2015**, *44*, 779–789; b) L. R. Holloway, P. M. Bogie, R. J. Hooley, *Dalton Trans.* **2017**, *46*, 14719–14723; c) W. M. Bloch, G. H. Clever, *Chem. Commun.* **2017**, *53*, 8506–8516.

[4] For selected examples see: a) D. A. McMorran, P. J. Steel, *Angew. Chem. Int. Ed.* **1998**, *37*, 3295–3297; b) D. K. Chand, K. Biradha, M. Fujita, *Chem. Commun.* **2001**, *1*, 1652–1653; c) G. H. Clever, S. Tashiro, M. Shionoya, *Angew. Chem. Int. Ed.* **2009**, *48*, 7010–7012; d) J. D. Crowley, E. L. Gavey, *Dalton Trans.* **2010**, *39*, 4035–4037; e) P. Liao, B. W. Langloss, A. M. Johnson, E. R. Knudsen, F. S. Tham, R. R. Julian, R. J. Hooley, *Chem. Commun.* **2010**, *46*, 4932–4934; f) N. Kishi, Z. Li, K. Yoza, M. Akita, M. Yoshizawa, *J. Am. Chem. Soc.* **2011**, *133*, 11438–11441; g) J. E. M. Lewis, E. L. Gavey, S. A. Cameron, J. D. Crowley, *Chem. Sci.* **2012**, *3*, 778–784; h) S. M. Jansze, M. D. Wise, A. V. Vologzhanina, R. Scopelliti, K. Severin, *Chem. Sci.* **2017**, *8*, 1901–1908; i) D. Preston, K. M. Patil, A. T. O'Neil, R. A. S. Vasdev, J. A. Kitchen, P. E. Kruger, *Inorg. Chem. Front.* **2020**, *7*, 2990–3001.

[5] a) D. Preston, J. E. Barnsley, K. C. Gordon, J. D. Crowley, *J. Am. Chem. Soc.* **2016**, *138*, 10578–10585; b) R. Zhu, W. M. Bloch, J. J. Holstein, S. Mandal, L. V. Schäfer, G. H. Clever, *Chem. - Eur. J.* **2018**, *24*, 12976–12982.

[6] a) W. M. Bloch, Y. Abe, J. J. Holstein, C. M. Wandtke, B. Dittrich, G. H. Clever, *J. Am. Chem. Soc.* **2016**, *138*, 13750–13755; b) W. M. Bloch, J. J. Holstein, W. Hiller, G. H. Clever, *Angew. Chem. Int. Ed.* **2017**, *56*, 8285–8289; c) K. Wu, B. Zhang, C. Drechsler, J. J. Holstein, G. H. Clever, *Angew. Chem. Int. Ed.* **2020**, DOI 10.1002/anie.202012425.

[7] a) S. Pullen, G. H. Clever, *Acc. Chem. Res.* **2018**, *51*, 3052–3064; b) D. Bardhan, D. K. Chand, *Chem. – Eur. J.*, **2019**, *25*, 12241-12269.

[8] a) S. Hiraoka, Y. Sakata, M. Shionoya, *J. Am. Chem. Soc.* **2008**, *130*, 10058–10059; b) H. Bin Wu, Q. M. Wang, *Angew. Chem. Int. Ed.* **2009**, *48*, 7343–7345; c) M. M. J. Smulders, A. Jiménez, J. R. Nitschke, *Angew. Chem. Int. Ed.* **2012**, *51*, 6681–6685; d) W. J. Ramsay, T. K. Ronson, J. K. Clegg, J. R. Nitschke, *Angew. Chem. Int. Ed.* **2013**, *52*, 13439–13443; e) K. Li, L. Y. Zhang, C. Yan, S. C. Wei, M. Pan, L. Zhang, C. Y. Su, *J. Am. Chem. Soc.* **2014**, *136*, 4456–4459; f) M. D. Wise, J. J. Holstein, P. Pattison, C. Besnard, E. Solari, R. Scopelliti, G. Bricogne, K. Severin, *Chem. Sci.* **2015**, *6*, 1004–1010; g) W. J. Ramsay, F. T. Szczypiński, H. Weissman, T. K. Ronson, M. M. J. Smulders, B. Rybtchinski, J. R. Nitschke, *Angew. Chem. Int. Ed.* **2015**, *54*, 5636–5640; h) S. Sanz, H. M. O'Connor, E. M. Pineda, K. S. Pedersen, G. S. Nichol, O. Mønsted, H. Weihe, S. Piligkos, E. J. L. McInnes, P. J. Lusby, E. K. Brechin, *Angew. Chem. Int. Ed.* **2015**, *54*, 6761–6764; i) A. J. Metherell, M. D. Ward, *Chem. Sci.* **2016**, *7*, 910–915; j) Y. J. Hou, K. Wu, Z. W. Wei, K. Li, Y. L. Lu, C. Y. Zhu, J. S. Wang, M. Pan, J. J. Jiang, G. Q. Li, C. Y. Su, *J. Am. Chem. Soc.* **2018**, *140*, 18183–18191; k) D. Preston, J. J. Sutton, K. C. Gordon, J. D. Crowley, *Angew. Chem. Int. Ed.* **2018**, *57*, 8659–8663; l) M. Hardy, N. Struch, J. J. Holstein, G. Schnakenburg, N. Wagner, M. Engeser, J. Beck, G. H. Clever, A. Lützen, *Angew. Chem. Int. Ed.* **2020**, *59*, 3195–3200; m) L. S. Lisboa, J. A. Findlay, L. J. Wright, C. G. Hartinger, J. D. Crowley, *Angew. Chem. Int. Ed.* **2020**, *59*, 11101–11107; n) D. Yang, J. L. Greenfield, T. K. Ronson, L. K. S. von Krbek, L. Yu, J. R. Nitschke, *J. Am. Chem. Soc.* **2020**, DOI 10.1021/jacs.0c09991.

[9] a) Y. Y. Zhang, W. X. Gao, L. Lin, G. X. Jin, *Coord. Chem. Rev.* **2017**, *344*, 323–344; b) M. Hardy, A. Lützen, *Chem. - Eur. J.* **2020**, *26*, 13332–13346.

[10] J. E. M. Lewis, A. Tarzia, A. J. P. White, K. E. Jelfs, *Chem. Sci.* **2020**, *11*, 677–683.

[11] a) S. Hiraoka, M. Fujita, *J. Am. Chem. Soc.* **1999**, *121*, 10239–10240; b) D. Ogata, J. Yuasa, *Angew. Chem. Int. Ed.* **2019**, *58*, 18424–18428; c) S. S. Mishra, S. V. K. Kompella, S. Krishnaswamy, S. Balasubramanian, D. K. Chand, *Inorg. Chem.* **2020**, *59*, 12884–12894.

[12] J. E. M. Lewis, J. D. Crowley, *ChemPlusChem* **2020**, *85*, 815–827.

[13] For selected examples see: a) N. Kamiya, M. Tominaga, S. Sato, M. Fujita, *J. Am. Chem. Soc.* **2007**, *129*, 3816–3817; b) T. Kikuchi, S. Sato, M. Fujita, *J. Am. Chem. Soc.* **2010**, *132*, 15930–15932; c) M. Ikemi, T. Kikuchi, S. Matsumura, K. Shiba, S. Sato, M. Fujita, *Chem. Sci.* **2010**, *1*, 68–71; d) J. Park, L. B. Sun, Y. P. Chen, Z. Perry, H. C. Zhou, *Angew. Chem. Int. Ed.* **2014**, *53*, 5842–5846; e) J. E. M. Lewis, A. B. S. Elliott, C. J. McAdam, K. C. Gordon, J. D. Crowley, *Chem. Sci.* **2014**, *5*, 1833–1843; f) K. K. G. Wong, N. Hoyas Pérez, A. J. P. White, J. E. M. Lewis, *Chem. Commun.* **2020**, *56*, 10453–10456.

[14] For selected examples see: a) M. Tominaga, K. Suzuki, T. Murase, M. Fujita, *J. Am. Chem. Soc.* **2005**, *127*, 11950–11951; b) S. Sato, J. Iida, K. Suzuki, M. Kawano, T. Ozeki, M. Fujita, *Science* **2006**, *313*, 1273–1276; c) K. Suzuki, M. Kawano, S. Sato, M. Fujita, *J. Am. Chem. Soc.* **2007**, *129*, 10652–10653; d) K. Suzuki, K. Takao, S. Sato, M. Fujita, *J. Am. Chem. Soc.* **2010**, *132*, 2544–2545; e) K. Suzuki, S. Sato, M. Fujita, *Nat. Chem.* **2010**, *2*, 25–29; f) D. Fujita, K. Suzuki, S. Sato, M. Yagi-Utsumi, Y. Yamaguchi, N. Mizuno, T. Kumasaka, M. Takata, M. Noda, S. Uchiyama, K. Kato, M. Fujita, *Nat. Commun.* **2012**, *3*, 1093; g) C. J. Bruns, D. Fujita, M. Hoshino, S. Sato, J. F. Stoddart, M. Fujita, *J. Am. Chem. Soc.* **2014**, *136*, 12027–12034; h) Y. Ueda, H. Ito, D. Fujita, M. Fujita, *J. Am. Chem. Soc.* **2017**, *139*, 6090–6093; i) L. R. Holloway, P. M. Bogie, Y. Lyon, C. Ngai, T. F. Miller, R. R. Julian, R. J. Hooley, *J. Am. Chem. Soc.* **2018**, *140*, 8078–8081.

[15] a) C. W. Tornøe, C. Christensen, M. Meldal, *J. Org. Chem.* **2002**, *67*, 3057–3064; b) V. V. Rostovtsev, L. G. Green, V. V. Fokin, K. B. Sharpless, *Angew. Chem. Int. Ed.* **2002**, *41*, 2596–2599.

[16] B. Schulze, U. S. Schubert, *Chem. Soc. Rev.* **2014**, *43*, 2522–2571.

[17] R. A. S. Vasdev, D. Preston, J. D. Crowley, *Dalton Trans.* **2017**, *46*, 2402–2414.

[18] a) D. Zhao, S. Tan, D. Yuan, W. Lu, Y. H. Rezenom, H. Jiang, L. Q. Wang, H. C. Zhou, *Adv. Mater.* **2011**, *23*, 90–93; b) J. E. M. Lewis, C. John McAdam, M. G. Gardiner, J. D. Crowley, *Chem. Commun.* **2013**, *49*, 3398–3400; c) A. B. S. Elliott, J. E. M. Lewis, H. Van Der Salm, C. J. McAdam, J. D. Crowley, K. C. Gordon, *Inorg. Chem.* **2016**, *55*, 3440–3447; d) S. K. Samanta, J. Quigley, B. Vinciguerra, V. Briken, L. Isaacs, *J. Am. Chem. Soc.* **2017**, *139*, 9066–9074.

[19] T. Cernak, K. D. Dykstra, S. Tyagarajan, P. Vachal, S. W. Krska, *Chem. Soc. Rev.* **2016**, *45*, 546–576.

[20] B. M. J. M. Suijkerbuijk, B. N. H. Aerts, H. P. Dijkstra, M. Lutz, A. L. Spek, G. Van Koten, R. J. M. Klein Gebbink, *Dalton Trans.* **2007**, 1273–1276.

[21] An exception to this is the work of Crowley and co-workers who observed dramatic differences in the kinetics of self-assembly with triazole-based ligands dependent upon the nature of the N-substituent: S. Ø. Scott, E. L. Gavey, S. J. Lind, K. C. Gordon, J. D. Crowley, *Dalton Trans.* **2011**, *40*, 12117-12124.

[22] a) A. M. Johnson, O. Moshe, A. S. Gamboa, B. W. Langloss, J. F. K. Limtiaco, C. K. Larive, R. J. Hooley, *Inorg. Chem.* **2011**, *50*, 9430–9442; b) M. Frank, L. Krause, R. Herbst-Irmer, D. Stalke, G. H. Clever, *Dalton Trans.* **2014**, *43*, 4587–4592; c) M. Frank, J. Ahrens, I. Bejenke, M. Krick, D. Schwarzer, G. H. Clever, *J. Am. Chem. Soc.* **2016**, *138*, 8279–8287; d) F. J. Rizzuto, M. Kieffer, J. R. Nitschke, *Chem. Sci.* **2018**, *9*, 1925–1930; e) M. Kieffer, R. A. Bilbeisi, J. D. Thoburn, J. K. Clegg, J. R. Nitschke, *Angew. Chem. Int. Ed.* **2020**, *59*, 11369–11373.